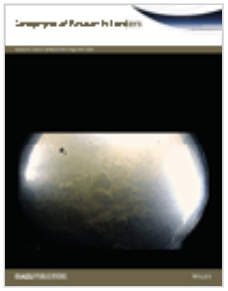

Volume 38, Issue 24

28 December 2011

Brief Detailed

Solid Earth

Surface wave tomography across Afar, Ethiopia: Crustal structure at a rift triple-junction zone

M. Guidarelli, G. Stuart, J. O. S. Hammond, J. M. Kendall, A. Ayele, M. Belachew

First Published: 30 December 2011 Vol: 38, L24313 | DOI: 10.1029/2011GL046840

KEY POINTS

- Study of the crustal structure at a rift triple-junction zone
- Surface wave tomography across the Afar
- Determination of shear wave velocity structure in Afar

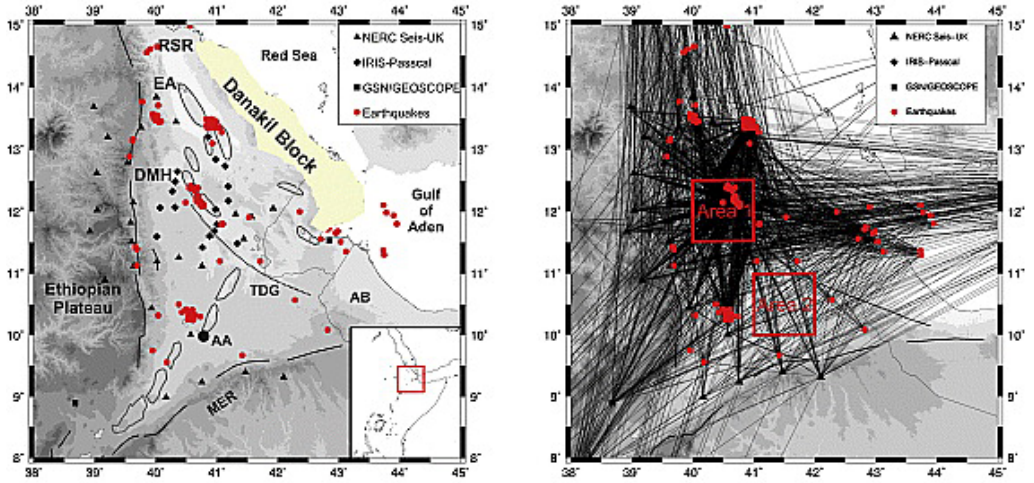

1 of 3

Imaging and modeling the ionospheric airglow response over Hawaii to the tsunami generated by the Tohoku earthquake of 11 March 2011

J. J. Makela, P. Lognonné, H. Hébert, T. Gehrels, L. Rolland, S. Allgeyer, A. Kherani, G. Occhipinti, E. Astafyeva, P. Coïsson, et al

First Published: 7 July 2011 Vol: 38, L00G02 | DOI: 10.1029/2011GL047860

KEY POINTS

- Coupling of the ocean surface to the upper atmosphere enables tsunami imaging

- The first ionospheric signature precedes the modeled ocean tsunami by one hour

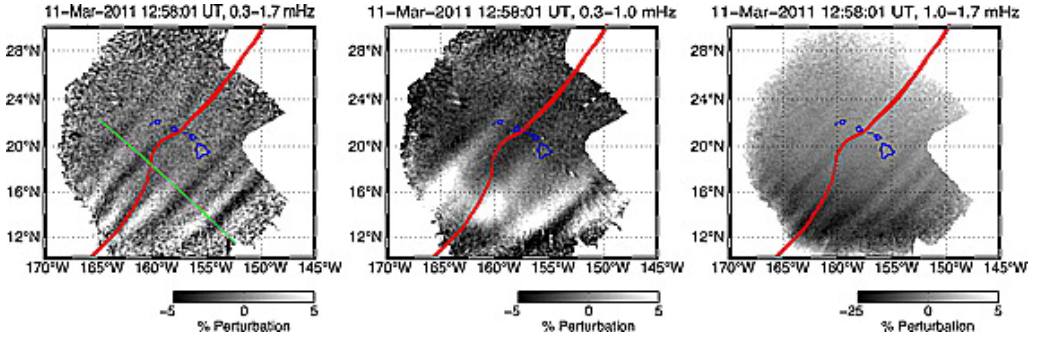

1 of 4

Retraction

WITHDRAWN: Correction to "Geomagnetic Semiannual Variation is not Overestimated and is not an Artifact of Systematic Solar Hemispheric Asymmetry"

L. Svalgaard

First Published: 30 December 2011 | DOI: 10.1029/2011GL049472

Solid Earth

Grüneisen parameter of hcp-Fe to 171 GPa

Caitlin A. Murphy, Jennifer M. Jackson, Wolfgang Sturhahn, Bin Chen

First Published: 20 December 2011 Vol: 38, L24306 | DOI: 10.1029/2011GL049531

KEY POINTS

- KeypointsMost accurate-to-date phonon DOS of iron up to 171 GPa gives γ_vib
- From the V-dependence of the phonon DOS, γ_vib0 = 2.0 ± 0.1 for q = 0.8 to 1.2
- From the same phonon DOS data, γ_vib is ~10% larger than γ_D at any given V

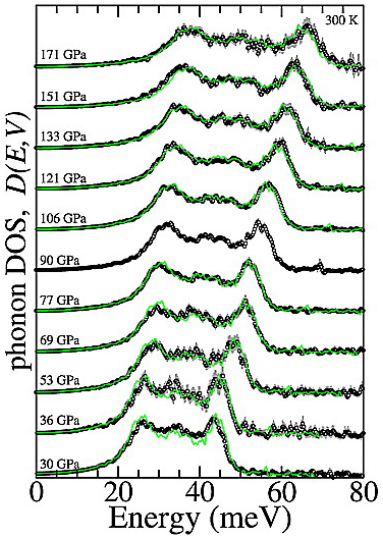

1 of 3

Earth's free oscillations recorded by free-fall OBS ocean-bottom seismometers at the Lesser Antilles subduction zone

A. Bécel, M. Laigle, J. Diaz, J.-P. Montagner, A. Hirn

First Published: 20 December 2011 Vol: 38, L24305 | DOI: 10.1029/2011GL049533

KEY POINTS

- Normal modes are recorded by free-fall broadband OBS for a M8.1 earthquake
- First time normal modes are measured on the ocean floor down to 1mHz
- It opens new horizons toward improving the long period seismic coverage of ocean

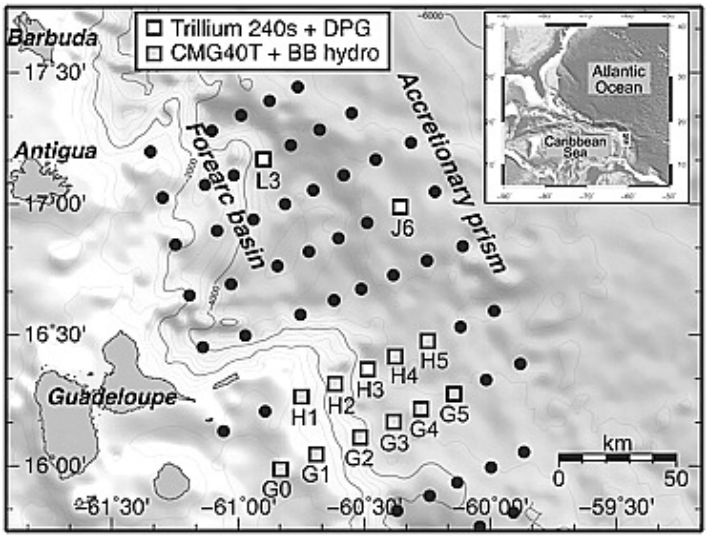

1 of 4

Atmospheric Science

Shortwave radiative closure experiment and direct forcing of dust aerosol over

northwestern China

J. M. Ge, J. P. Huang, J. Su, J. R. Bi, Q. Fu

First Published: 20 December 2011 Vol: 38, L24803 | DOI: 10.1029/2011GL049571

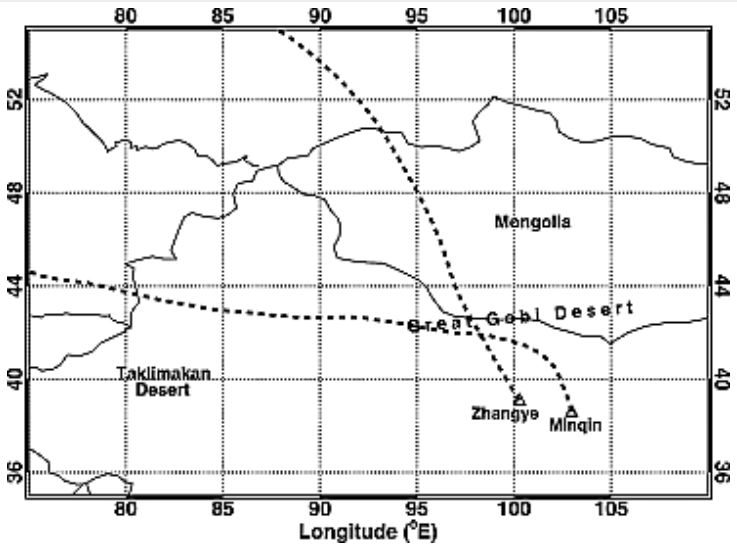

1 of 4

Planets

Comparison of Titan's north polar lakes with terrestrial analogs

Priyanka Sharma, Shane Byrne

First Published: 22 December 2011 Vol: 38, L24203 | DOI: 10.1029/2011GL049577

KEY POINTS

- We compared lakes on Earth and Titan using Cassini RADAR and SRTM data
- Diverse terrestrial processes produce statistically different shorelines
- We calculated fractal dimension, shoreline development index & elongation index

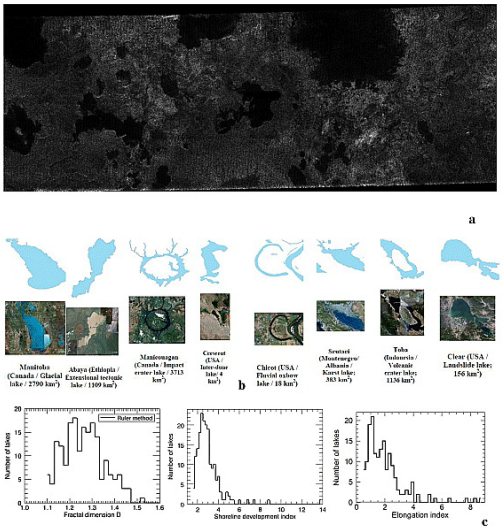

1 of 2

Space Sciences

Modeling 1 AU solar wind observations to estimate azimuthal magnetic fields at the solar source surface

Hagen Schulte in den Bäumen, Iver H. Cairns, P. A. Robinson

First Published: 17 December 2011 Vol: 38, L24101 | DOI: 10.1029/2011GL049578

KEY POINTS

- Nonzero azimuthal magnetic fields are found at the photosphere
- Non-Parker-like magnetic fields at 1 AU can be explained naturally
- Our results lead to important consequences for the distant heliospheric field

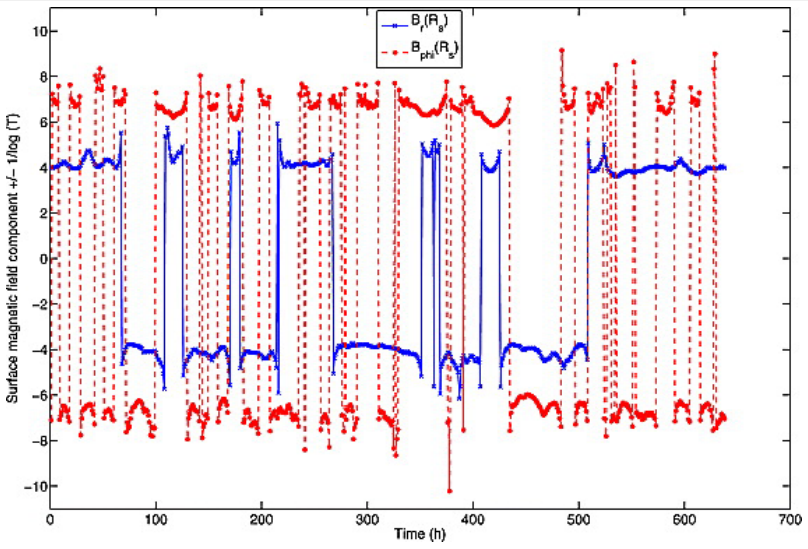

1 of 4

Planets

Testing for flow in the north polar layered deposits of Mars using radar stratigraphy and a simple 3D ice-flow model

N. B. Karlsson, J. W. Holt, R. C. A. Hindmarsh

First Published: 22 December 2011 Vol: 38, L24204 | DOI: 10.1029/2011GL049630

KEY POINTS

- First 3D modeling of internal layers in the north polar layered deposits, Mars
- First comparison between observed radar data and modeled layers
- Results show no compelling evidence for ice flow having occurred

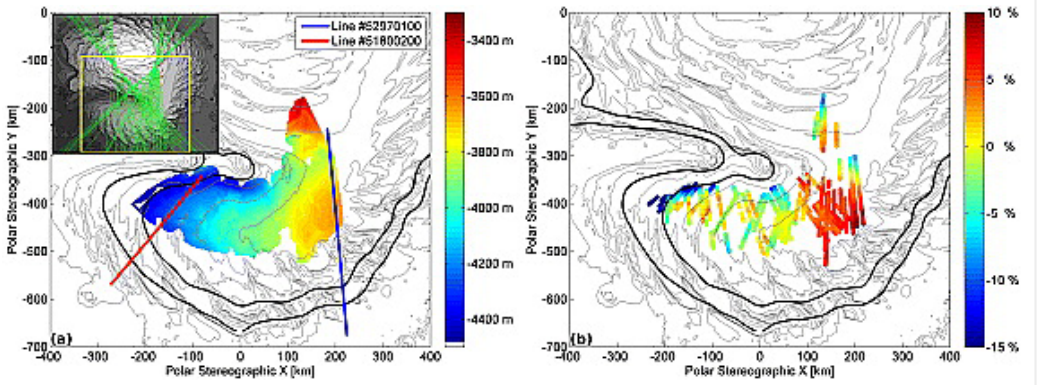

1 of 4

Solid Earth

Dynamics of a lava fountain revealed by geophysical, geochemical and thermal satellite measurements: The case of the 10 April 2011 Mt Etna eruption

A. Bonaccorso, T. Caltabiano, G. Currenti, C. Del Negro, S. Gambino, G. Ganci, S. Giammanco, F. Greco, A. Pistorio, G. Salerno, et al

First Published: 22 December 2011 Vol: 38, L24307 | DOI: 10.1029/2011GL049637

KEY POINTS

- Multidisciplinary approach tracks the dynamics of a lava fountain
- Satellite thermal data give constraints on the total erupted volume
- SO2 flux measurements provide insight on the degassed magma volume

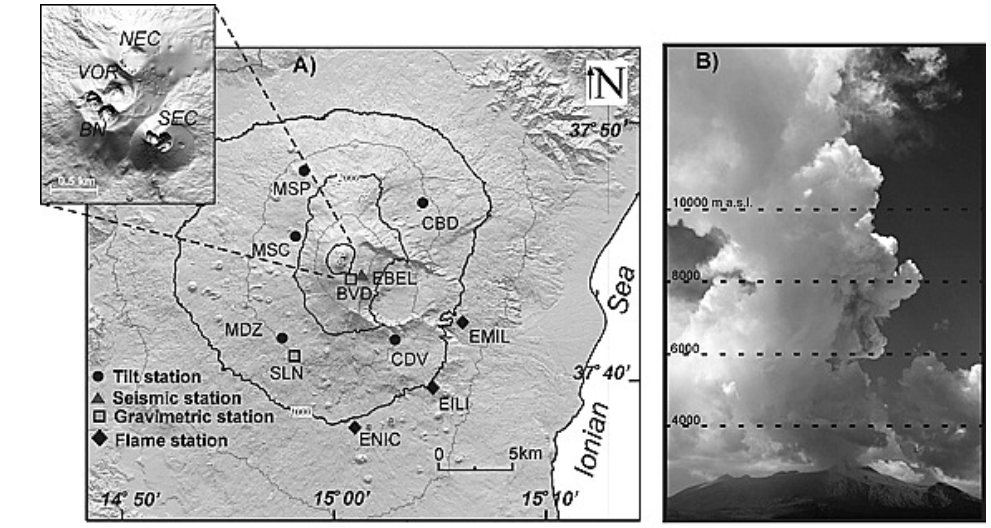

1 of 3

Climate

Response of a marine-terminating Greenland outlet glacier to abrupt cooling 8200 and 9300 years ago

Nicolás E. Young, Jason P. Briner, Yarrow Axford, Beata Csatho, Greg S. Babonis, Dylan H. Rood, Robert C. Finkel

First Published: 16 December 2011 Vol: 38, L24701 | DOI: 10.1029/2011GL049639

KEY POINTS

- GrIS outlet glaciers responded to the 9.3 and 8.2 ka cooling events
- GrIS outlet glaciers track temperature change with minimal lag times
- In addition to quick retreat, GrIS outlets can also advance rapidly

Highlight

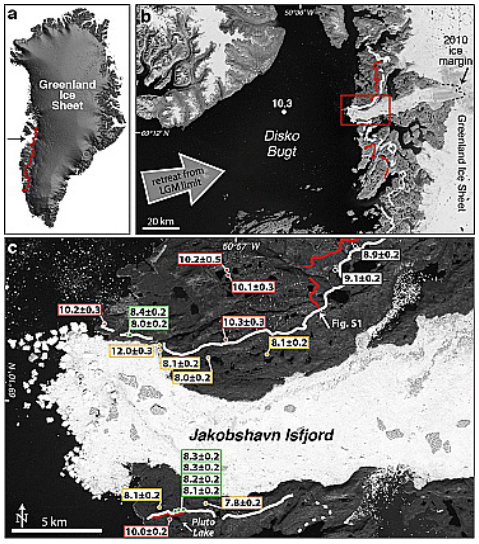

1 of 3

Space Sciences

Advection of magnetic energy as a source of power for auroral arcs

D. J. Knudsen, J. K. Burchill, E. F. Donovan, V. M. Uritsky

First Published: 21 December 2011 Vol: 38, L24103 | DOI: 10.1029/2011GL049661

KEY POINTS

- Plasma convection across current sheets carries magnetic energy
- Magnetic energy advection can feed auroral arcs indefinitely
- This mechanism may have broad application

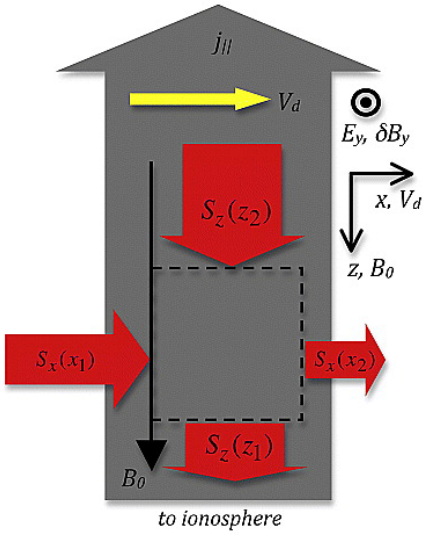

1 of 3

Atmospheric Science

Vertical dependence of black carbon, sulphate and biomass burning aerosol radiative forcing

Bjørn H. Samset, Gunnar Myhre

First Published: 16 December 2011 Vol: 38, L24802 | DOI: 10.1029/2011GL049697

KEY POINTS

- Black carbon has significant vertical sensitivity even in the absence of clouds
- Profiles must be considered also for sulphate and biomass burning aerosols
- The strong BC sensitivity can cause intermodel differences even for low loads

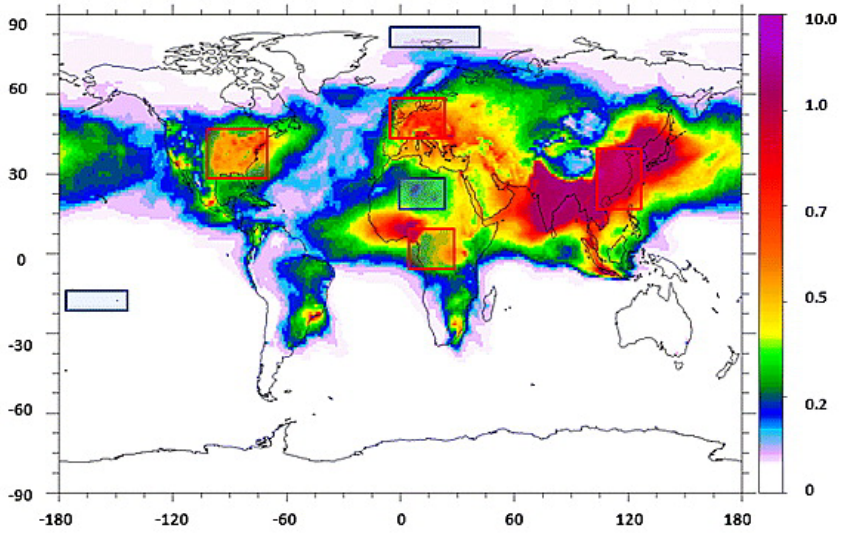

1 of 6

Oceans

Western Arctic Ocean temperature variability during the last 8000 years

Jesse R. Farmer, Thomas M. Cronin, Anne de Vernal, Gary S. Dwyer, Lloyd D. Keigwin, Robert C. Thunell

First Published: 17 December 2011 Vol: 38, L24602 | DOI: 10.1029/2011GL049714

KEY POINTS

- Periods of reduced sea ice correspond with increased Atlantic Layer temperature
- The modern thermal structure of the western Arctic Ocean has existed since 7 ka
- Modern-day Atlantic Layer temperatures are the warmest of the past millennium

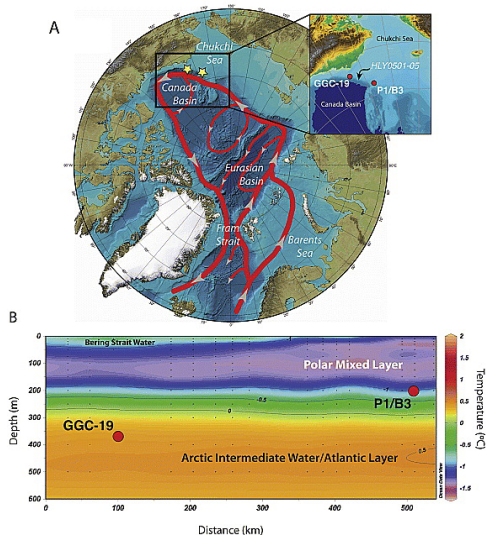

1 of 3

Solid Earth

Deep structure of lithospheric fault zones

J. P. Platt, W. M. Behr

First Published: 21 December 2011 Vol: 38, L24308 | DOI: 10.1029/2011GL049719

KEY POINTS

- Calculation of the cumulative width of plate boundary faults at depth
- Stress in the lithosphere is controlled by the strength of intact rock
- Fault zone width is controlled by the rheology of damaged material

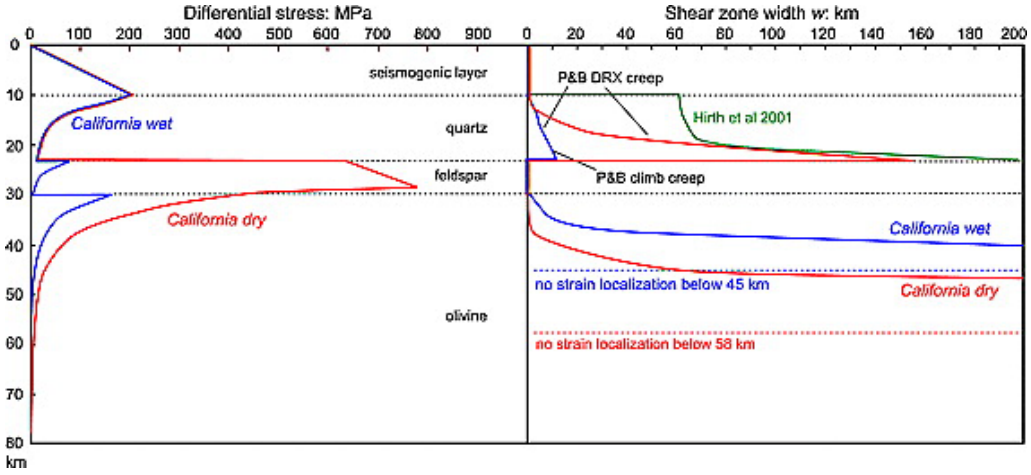

1 of 2

Oceans

Chemoautotrophy in the ocean

Jack J. Middelburg

First Published: 23 December 2011 Vol: 38, L24604 | DOI: 10.1029/2011GL049725

KEY POINTS

- Chemoautotrophy totals 0.79 Pg C per year
- Sediments and nitrifiers in the water column dominate chemoautotrophy
- Chemoautotrophy matters for the carbon cycle and marine food webs

Highlight

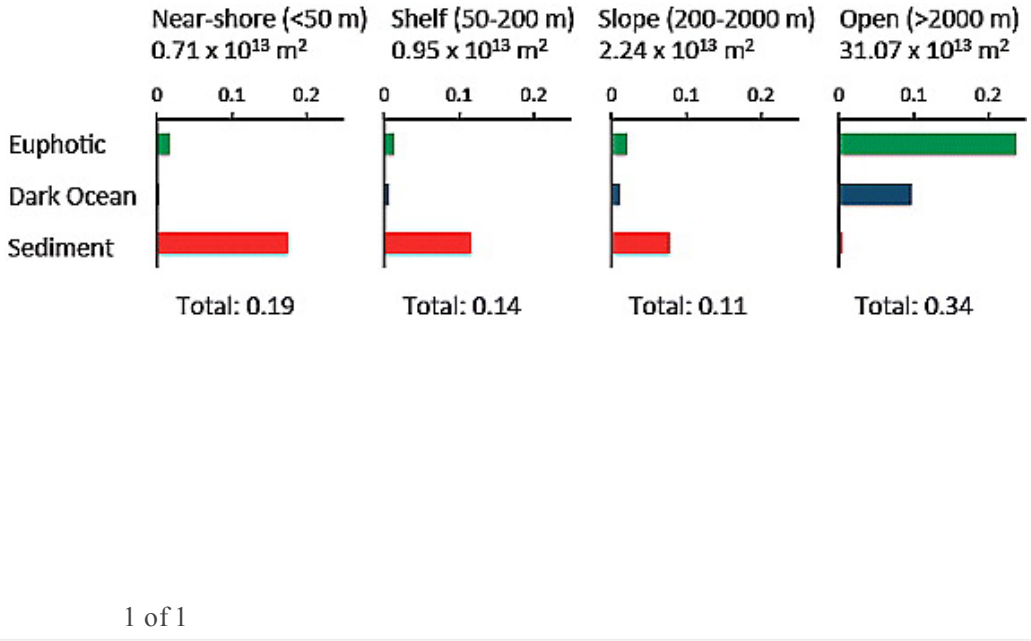

1 of 1

Atmospheric Science

Migrating source of energetic radiation generated by thunderstorm activity

Tatsuo Torii, Takeshi Sugita, Masashi Kamogawa, Yasuyuki Watanabe, Kenichi Kusunoki

First Published: 16 December 2011 Vol: 38, L24801 | DOI: 10.1029/2011GL049731

KEY POINTS

- Emission of energetic radiation without lightning
- Identified location of migrating source of energetic radiation

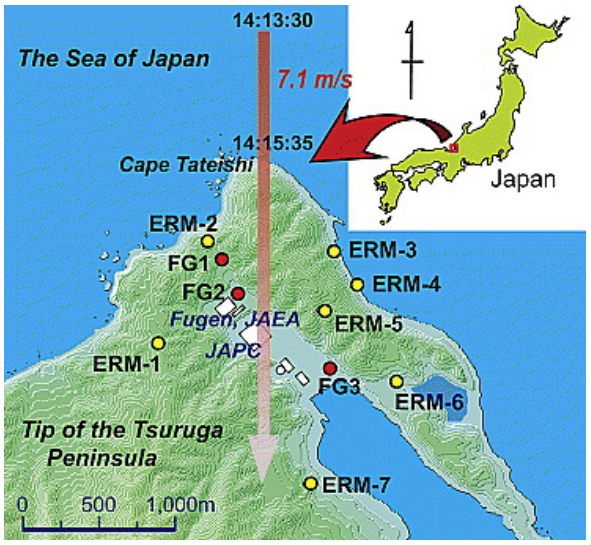

1 of 7

Hydrology and Land Surface Studies

Sorted bedform pattern evolution: Persistence, destruction and self-organized intermittency

Evan B. Goldstein, A. Brad Murray, Giovanni Coco

First Published: 23 December 2011 Vol: 38, L24402 | DOI: 10.1029/2011GL049732

KEY POINTS

- Pattern maturation processes lead to pattern destruction or intermittency
- Spatial and temporal intermittence in patterns occurs under uniform forcing
- Modeled behaviors could explain observed morphologies and degrees of persistence

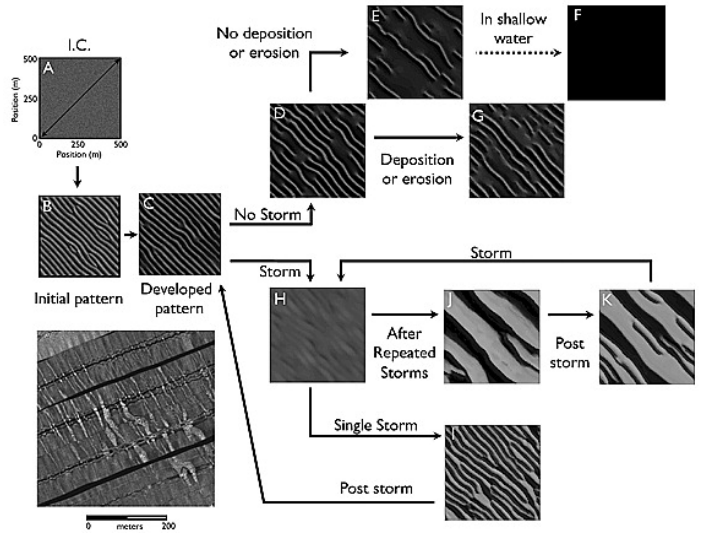

1 of 2

Solid Earth

Variations of crustal elastic properties during the 2009 L'Aquila earthquake inferred from cross-correlations of ambient seismic noise

L. Zaccarelli, N. M. Shapiro, L. Faenza, G. Soldati, A. Michelini

First Published: 17 December 2011 Vol: 38, L24304 | DOI: 10.1029/2011GL049750

KEY POINTS

- Seismic velocities in the Earth crust are reduced after the L'Aquila earthquake
- Velocity reduction is caused by co-seismic shaking of shallow soft layers
- Noise correlations provide robust information about tiny crustal variations

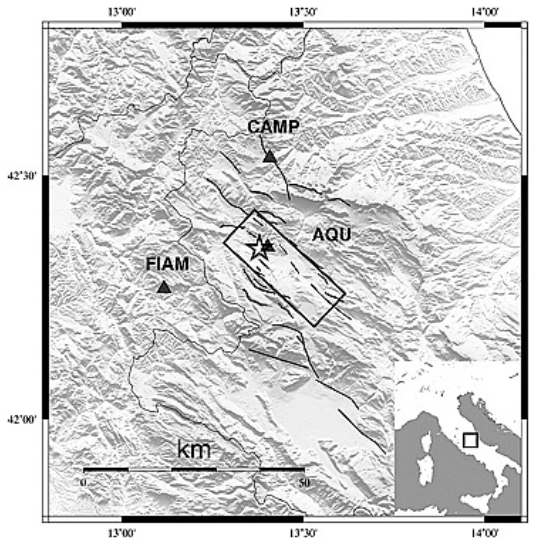

1 of 3

Climate

Stratospheric heating by potential geoengineering aerosols

A. J. Ferraro, E. J. Highwood, A. J. Charlton-Perez

First Published: 28 December 2011 Vol: 38, L24706 | DOI: 10.1029/2011GL049761

KEY POINTS

- Geoengineering aerosols change stratospheric radiative heating rates
- Heating rates depend on aerosol species and size

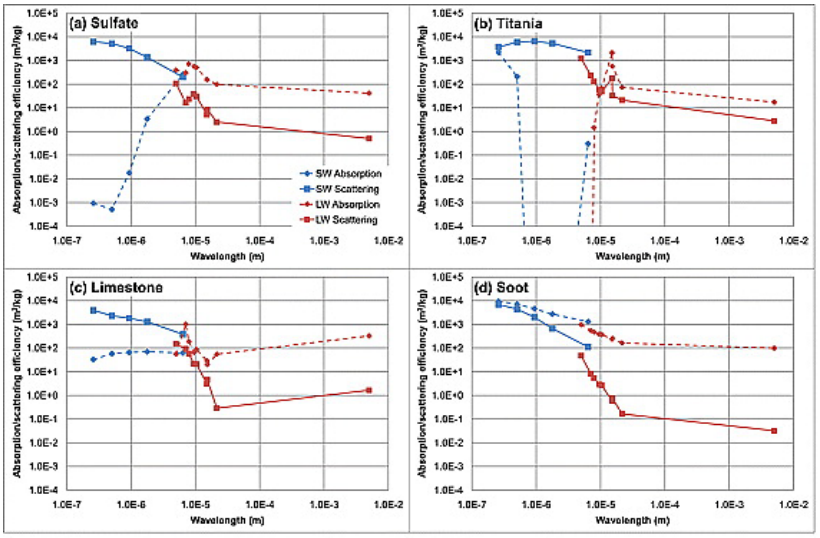

1 of 3

Solid Earth

Interseismic strain accumulation across the Manyi fault (Tibet) prior to the 1997 M_w 7.6 earthquake

M. A. Bell, J. R. Elliott, B. E. Parsons

First Published: 16 December 2011 Vol: 38, L24302 | DOI: 10.1029/2011GL049762

KEY POINTS

- The Manyi fault was accumulating strain at 3 mm/yr prior to the 1997 earthquake
- This small rate means the current deformation is due to postseismic processes
- No slip is observed on the potential westward extension of the Kunlun fault

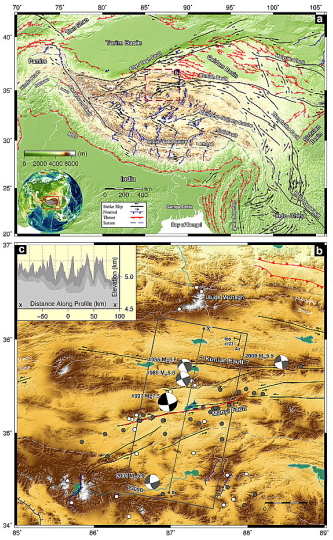

1 of 3

Atmospheric Science

Solar irradiance, cosmic rays and cloudiness over daily timescales

Benjamin A. Laken, Jasa Čalogović

First Published: 29 December 2011 Vol: 38, L24811 | DOI: 10.1029/2011GL049764

KEY POINTS

- Rigorous statistical analysis and sample construction
- Cloud examined over range of regions and conditions
- Solar activity not correlated to widespread cloud changes

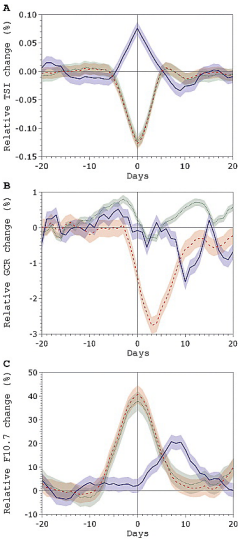

1 of 2

Oceans

CO_2 uptake in the East China Sea relying on Changjiang runoff is prone to change

Chun-Mao Tseng, K.-K. Liu, G.-C. Gong, P.-Y. Shen, W.-J. Cai
First Published: 31 December 2011 Vol: 38, L24609 | DOI: 10.1029/2011GL049774

KEY POINTS

- Strong control of river runoff on the CO2 uptake capacity change in ECS
- The threat of the ECS shifting from a sink of atmospheric CO2 to a source
- Changjiang discharge decreases, resulting in the ECS CO2 uptake reduction

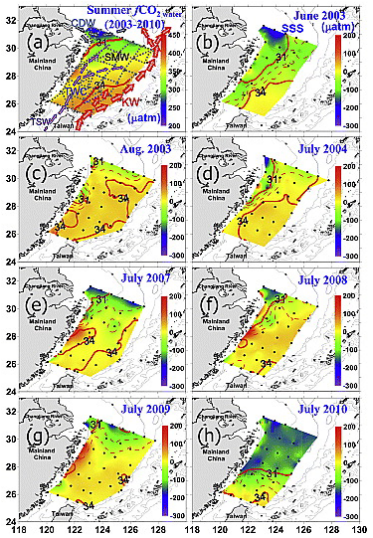

1 of 4

Atmospheric Science

Arctic winter 2010/2011 at the brink of an ozone hole

B.-M. Sinnhuber, G. Stiller, R. Ruhnke, T. von Clarmann, S. Kellmann, J. Aschmann
First Published: 30 December 2011 Vol: 38, L24814 | DOI: 10.1029/2011GL049784

KEY POINTS

- Large losses of Arctic stratospheric ozone were observed during winter 2010/11
- A further cooling of 1K would have resulted in locally near-complete ozone loss
- A 1K cooling can counterbalance a 10% reduction in halogens

Highlight

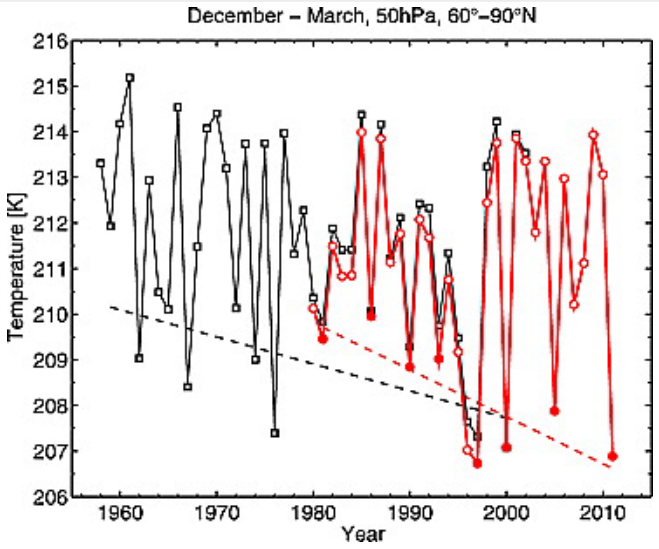

1 of 3

Solid Earth

Phase transition and metallization of FeO at high pressures and temperatures

Rebecca A. Fischer, Andrew J. Campbell, Oliver T. Lord, Gregory A. Shofner, Przemyslaw Dera, Vitali B. Prakapenka

First Published: 16 December 2011 Vol: 38, L24301 | DOI: 10.1029/2011GL049800

KEY POINTS

- FeO becomes metallic at P-T conditions of the Earth's lower mantle and core
- This new phase boundary resolves major discrepancies in the FeO phase diagram

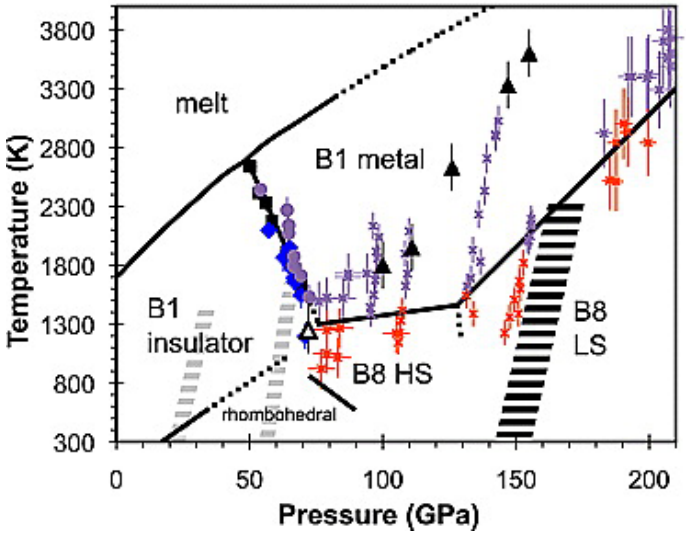

1 of 4

Oceans

Observation of decadal change in the Atlantic meridional overturning circulation using 10 years of continuous transport data

Uwe Send, Matthias Lankhorst, Torsten Kanzow

First Published: 24 December 2011 Vol: 38, L24606 | DOI: 10.1029/2011GL049801

KEY POINTS

- Data suggest a weakening Atlantic MOC by 20% over 10 years
- Interannual/decadal transport variability concentrated in Labrador Sea Water
- Suggestions of similar recent decrease and some meridional coherence in models

Open Access Highlight

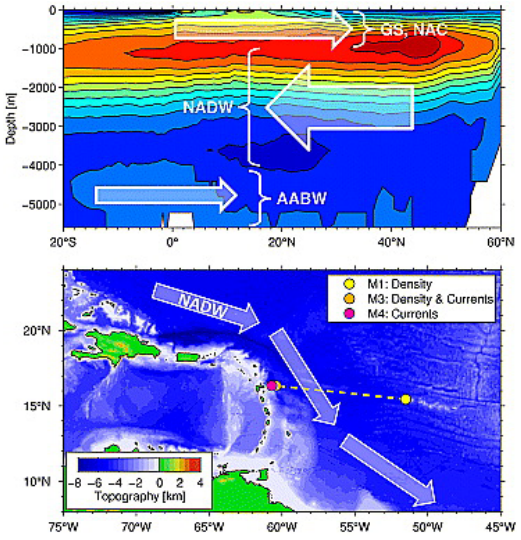

1 of 4

Planets

Measurements of Martian dust devil winds with HiRISE

D. S. Choi, C. M. Dundas

First Published: 31 December 2011 Vol: 38, L24206 | DOI: 10.1029/2011GL049806

KEY POINTS

- We measure dust devil winds from HiRISE images by tracking cloud features
- 20-30 m/s winds are typical; some areas exhibit strong tangential motion
- Solid body rotation present within core, but we cannot confirm Rankine profile

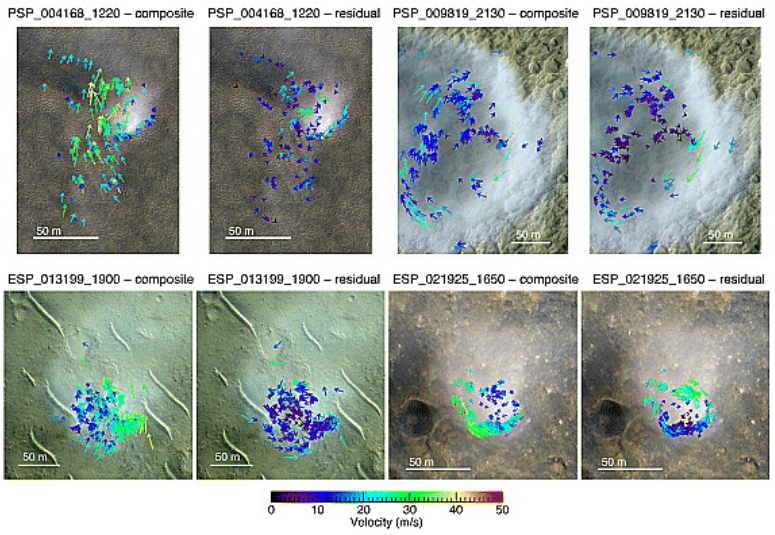

1 of 3

Climate

On the observational assessment of climate model performance

J. D. Annan, J. C. Hargreaves, K. Tachiiri

First Published: 17 December 2011 Vol: 38, L24702 | DOI: 10.1029/2011GL049812

KEY POINTS

- We present an alternative paradigm for ensemble evaluation
- Previous assessments of CMIP3 ensemble spread may be misleadingly pessimistic

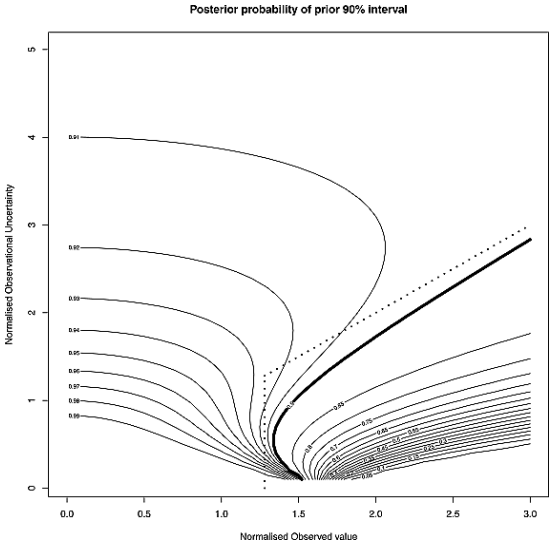

1 of 2

Oceans

Buffered versus non-buffered ocean carbon reservoir variations: Application to the sensitivity of atmospheric pCO_2 to ocean circulation changes

M. d'Orgeville, M. H. England, W. P. Sijp

First Published: 21 December 2011 Vol: 38, L24603 | DOI: 10.1029/2011GL049823

KEY POINTS

- How to understand impacts of ocean circulation changes on atmospheric CO2
- New diagnostic of changes in the buffered and non-buffered ocean C reservoirs
- Key role of variations in surface alkalinity, temperature and salinity

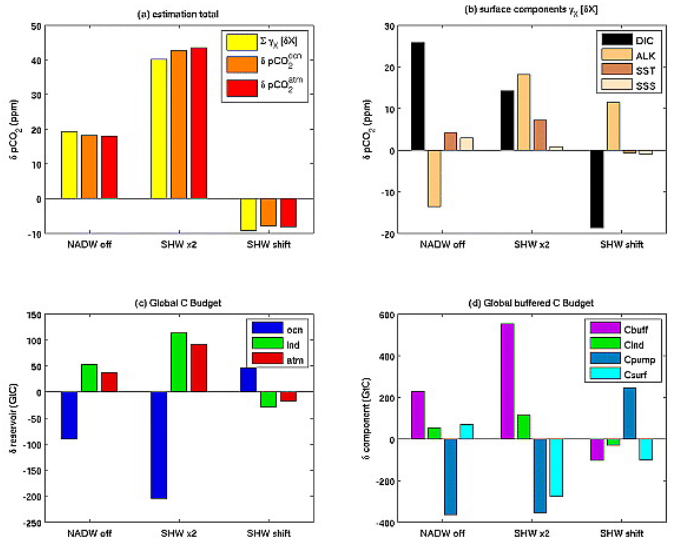

1 of 2

Solid Earth

A new sedimentary benchmark for the Deccan Traps volcanism?

Eric Font, Anne Nédélec, Brooks B. Ellwood, José Mirão, Pedro F. Silva

First Published: 23 December 2011 Vol: 38, L24309 | DOI: 10.1029/2011GL049824

KEY POINTS

- We found a low MS and Cl-bearing interval just below the KPB
- Magnetic signal is carried by an enigmatic Cl-iron oxide similar to hematite
- We hypothesize that it was formed during a major volcanic pulse of the Deccan

1 of 4

Hydrology and Land Surface Studies

Contribution of peat compaction to relative sea-level rise within Holocene deltas

S. van Asselen, D. Karssenberg, E. Stouthamer

First Published: 20 December 2011 Vol: 38, L24401 | DOI: 10.1029/2011GL049835

KEY POINTS

- Subsidence due to peat compaction highly depends on sequence build-up
- Compaction rates averaged over long periods may underestimate current rates
- (Peat compaction) models should be calibrated using an extensive field dataset

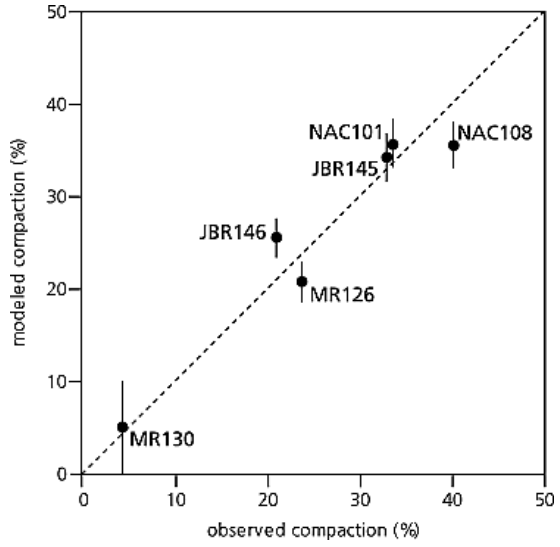

1 of 5

Oceans

Ocean wave conditions in the Chukchi Sea from satellite and *in situ* observations

Oceana P. Francis, Gleb G. Panteleev, David E. Atkinson

First Published: 31 December 2011 Vol: 38, L24610 | DOI: 10.1029/2011GL049839

KEY POINTS

- Significant wave height increase in the Arctic
- Ocean wave satellite altimetry and in situ observations correlating
- Wave increase due to sea ice decline

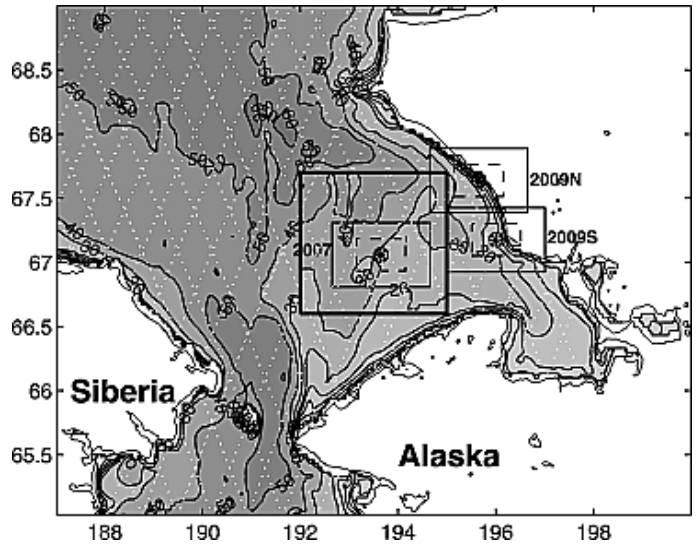

1 of 4

Planets

Detecting tides and gravity at Europa from multiple close flybys

Ryan S. Park, Sami W. Asmar, Brent B. Buffington, Bruce Bills, Stefano Campagnola, Paul W. Chodas, William M. Folkner, Alex S. Konopliv, Anastassios E. Petropoulos

First Published: 21 December 2011 Vol: 38, L24202 | DOI: 10.1029/2011GL049842

KEY POINTS

- Detecting Europa tides from multiple flybys
- Detecting Europa gravity from multiple flybys
- Constraint on the existence of subsurface ocean using Ka-band tracking

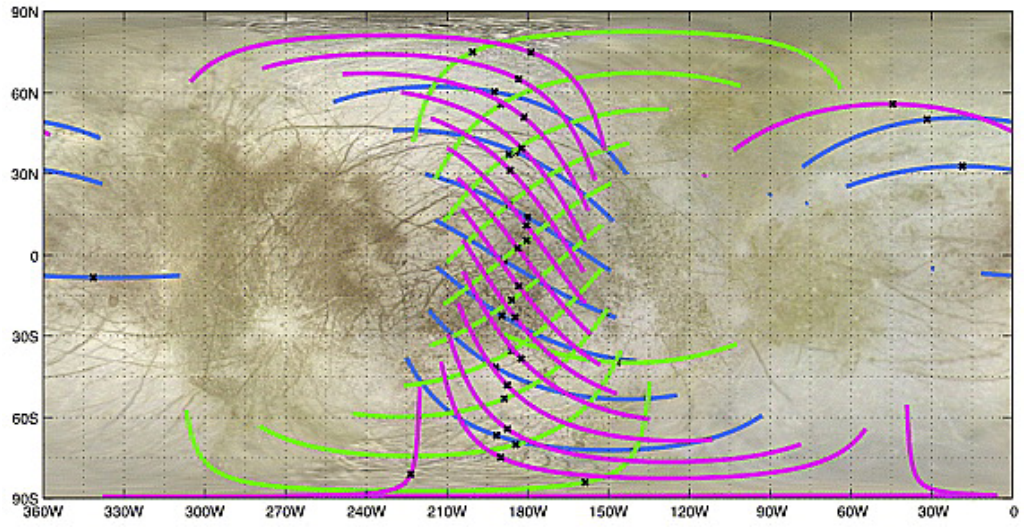

1 of 3

The Cryosphere

In-situ quantification of ice rheology and direct measurement of the Raymond Effect at Summit, Greenland using a phase-sensitive radar

Fabien Gillet-Chaulet, Richard C. A. Hindmarsh, Hugh F. J. Corr, Edward C. King, Adrian Jenkins

First Published: 31 December 2011 Vol: 38, L24503 | DOI: 10.1029/2011GL049843

KEY POINTS

- Most accurate field quantification of ice rheology so far
- First direct demonstration of Raymond effect
- Demonstration that laboratory ice studies do not explore full range of ice flow

Highlight

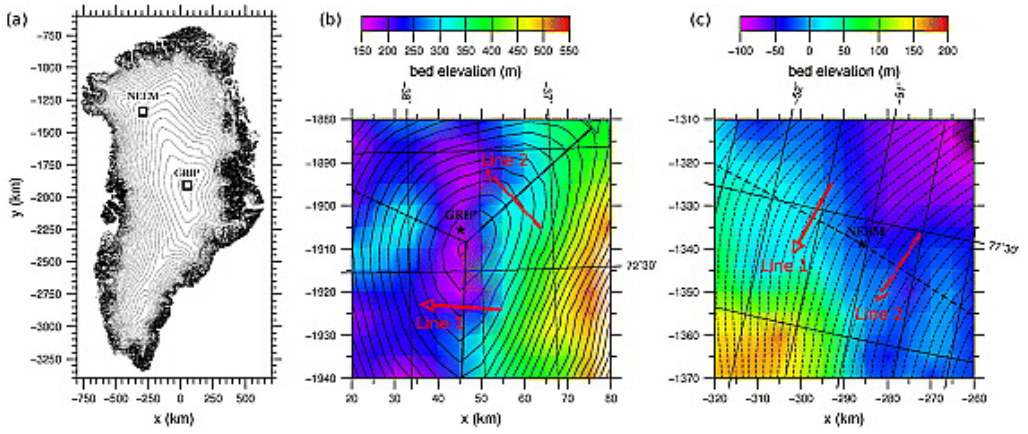

1 of 3

Solid Earth

Absolute gravity calibration of GPS velocities and glacial isostatic adjustment in mid-continent North America

S. Mazzotti, A. Lambert, J. Henton, T. S. James, N. Courtier

First Published: 28 December 2011 Vol: 38, L24311 | DOI: 10.1029/2011GL049846

KEY POINTS

- Integration of absolute gravity and GPS data
- Constraints to the ITRF and GPS rate alignment
- Usability of GPS rates for postglacial rebound and sea-level studies

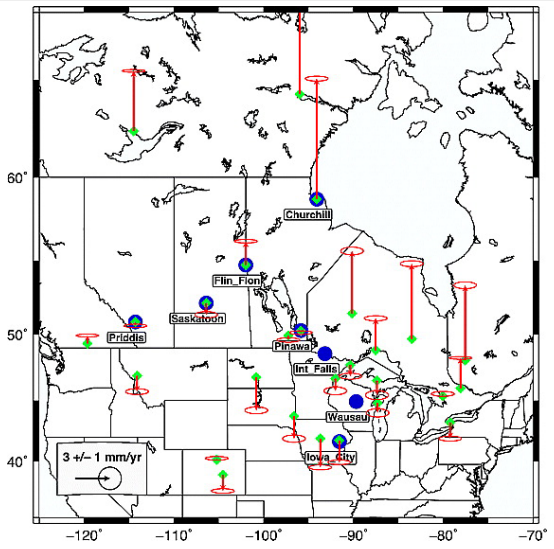

1 of 3

Oceans

Surface water dissolved aluminum and titanium: Tracers for specific time scales of dust deposition to the Atlantic?

Anna Dammshäuser, Thibaut Wagener, Peter L. Croot

First Published: 17 December 2011 Vol: 38, L24601 | DOI: 10.1029/2011GL049847

KEY POINTS

- Dissolved Al and Ti are specifically related to dust deposition in the Atlantic
- Both metals may serve to trace specific time scales of dust deposition
- Al and Ti show specific spatial variations in dissolution and removal processes

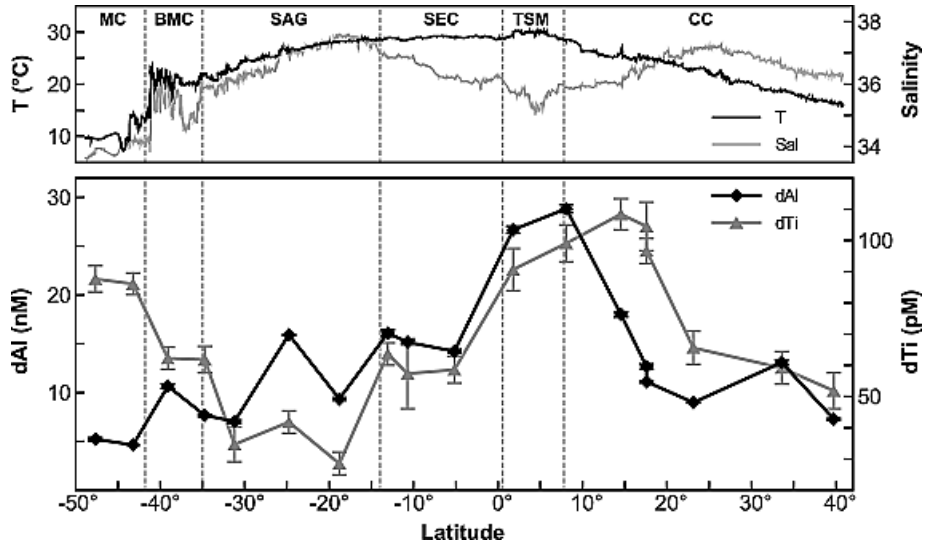

1 of 2

Atmospheric Science

Implications of extinction due to meteoritic smoke in the upper stratosphere

Ryan R. Neely III, Jason M. English, Owen B. Toon, Susan Solomon, Michael Mills, Jeffery P. Thayer

First Published: 23 December 2011 Vol: 38, L24808 | DOI: 10.1029/2011GL049865

KEY POINTS

- Meteoritic smoke dominates aerosol extinction in the upper stratosphere
- Meteoritic smoke influences aerosol properties throughout the stratosphere
- Extinction retrievals of the stratosphere should consider meteoritic smoke

Open Access

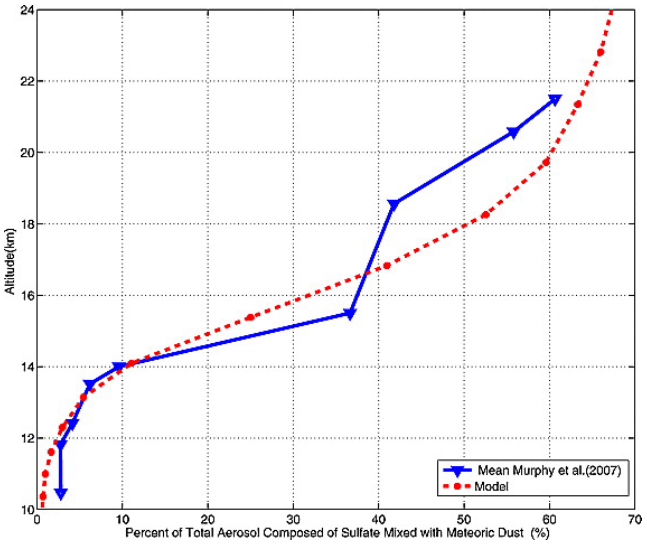

1 of 4

Ionospheric effects of whistler waves from rocket-triggered lightning

B. R. T. Cotts, M. Gołkowski, R. C. Moore

First Published: 24 December 2011 Vol: 38, L24805 | DOI: 10.1029/2011GL049869

KEY POINTS

- The spectral content of lightning affects the characteristics of LEP events
- Lightning with higher ELF content precipitates electrons at higher L-shells
- ELF frequencies precipitate electrons more efficiently than VLF frequencies

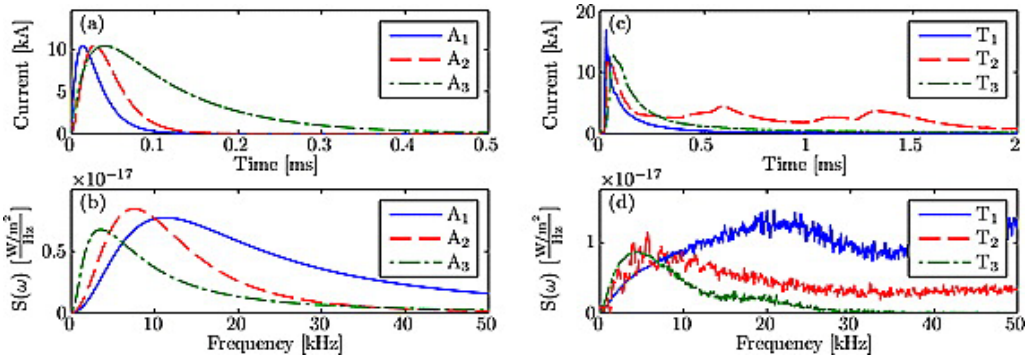

1 of 4

Climate

Footprints of IOD and ENSO in the Kenyan coral record

Nobuko Nakamura, Hajime Kayanne, Hiroko Iijima, Timothy R. McClanahan, Swadhin K. Behera, Toshio Yamagata

First Published: 31 December 2011 Vol: 38, L24708 | DOI: 10.1029/2011GL049877

KEY POINTS

- Kenyan coral record does not show the ENSO-induced seasonal signals clearly
- Kenyan coral records IOD and pre-El Nino signals
- The cold SST condition before El Nino was prominent in the last 19th century

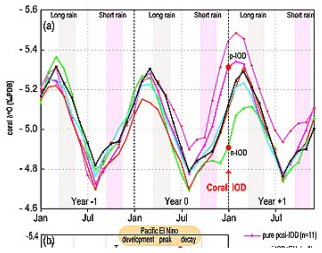

1 of 2

Atmospheric Science

The impact of the Madden-Julian Oscillation trend on the Arctic amplification of surface air temperature during the 1979–2008 boreal winter

Changhyun Yoo, Steven Feldstein, Sukyoung Lee

First Published: 20 December 2011 Vol: 38, L24804 | DOI: 10.1029/2011GL049881

KEY POINTS

- Interdecadal changes in Madden-Julian Oscillation influence polar amplification
- Intraseasonal processes influence interdecadal variability
- Poleward Rossby wave propagation warms Arctic

1 of 4

Oceans

Nonlinear internal tidal waves in a semi-enclosed sea (Gulf of California)

Vadim Novotryasov, Anatoliy Filonov, Miguel F. Lavín

First Published: 31 December 2011 Vol: 38, L24611 | DOI: 10.1029/2011GL049886

KEY POINTS

- Highly nonlinear internal tide in Gulf of California
- An analytical model spectrum of nonlinear internal tidal waves
- The internal tide in the northern Gulf of California is a cubically nonlinear

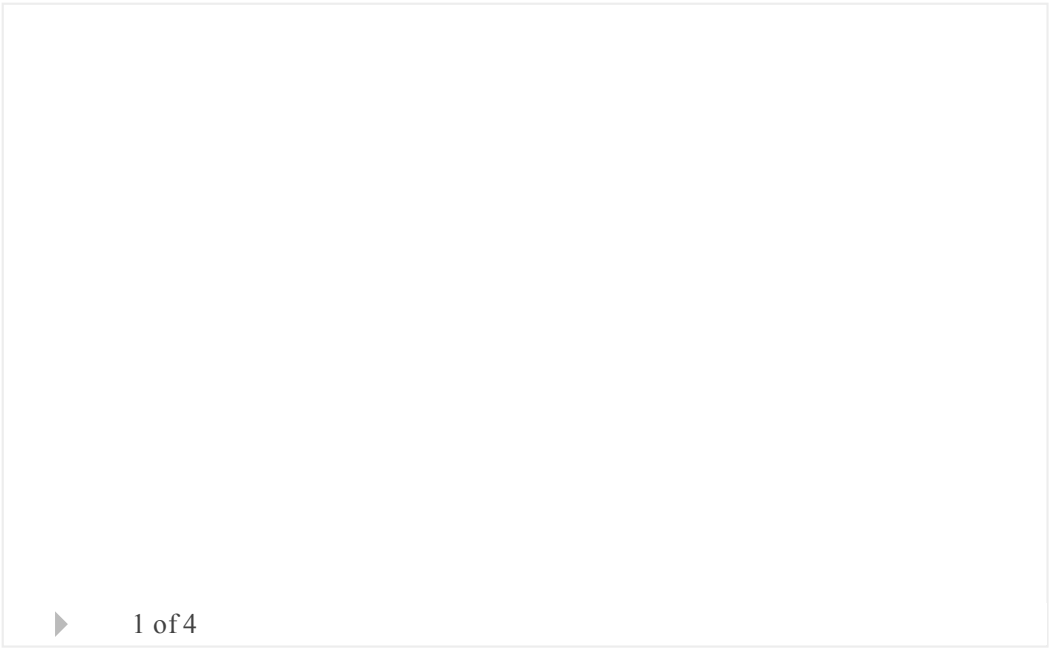

1 of 4

Solid Earth

Role of drainage conditions in deformation and fracture of porous rocks under triaxial compression in the laboratory

Xinglin Lei, Tetsuya Tamagawa, Kazuhiko Tezuka, Manabu Takahashi

First Published: 28 December 2011 Vol: 38, L24310 | DOI: 10.1029/2011GL049888

KEY POINTS

- Dilatancy-hardening can be greatly suppressed by dilatancy-driven fluid flow
- Good drainage conditions can to enlarge fault nucleation dimension and duration
- Decreasing pore pressure due to dilatancy may enhance the formation of CBs

1 of 5

Planets

Quantification of the dry history of the Martian soil inferred from in situ microscopy

W. T. Pike, U. Staufer, M. H. Hecht, W. Goetz, D. Parrat, H. Sykulska-Lawrence, S. Vijendran, M. B. Madsen

First Published: 21 December 2011 Vol: 38, L24201 | DOI: 10.1029/2011GL049896

KEY POINTS

- Particle size distribution performed on martian soil sample from Phoenix site
- Fractal analysis indicates nonaqueous formation (deficient in fines)
- At least two populations of particles, sorted by transport processes

1 of 3

Atmospheric Science

Global CO_2fluxes inferred from surface air-sample measurements and from TCCON retrievals of the CO_2 total column

F. Chevallier, N. M. Deutscher, T. J. Conway, P. Ciais, L. Ciattaglia, S. Dohe, M. Fröhlich, A. J. Gomez-Pelaez, D. Griffith, F. Hase, et al

First Published: 29 December 2011 Vol: 38, L24810 | DOI: 10.1029/2011GL049899

KEY POINTS

- Consistent seasonal cycle inferred from XCO2 and from pointwise observations
- The TCCON inversion improves the quality of the prior fluxes
- Our study experimentally confirms the usefulness of space-borne CO2 monitoring

1 of 3

Oceans

Locally enhanced wintertime air-sea interaction and deep oceanic mixed layer formation associated with the subarctic front in the North Pacific

Hiroyuki Tomita, Shinya Kouketsu, Eitarou Oka, Masahisa Kubota

First Published: 22 December 2011 Vol: 38, L24607 | DOI: 10.1029/2011GL049902

KEY POINTS

- Air-sea process due to sub-arctic front enhances ocean heat loss and mixing
- Enhanced ocean heat loss and wind mixing selectively forms deep mixed layer
- Produced deep ocean mixed layers are the source of Transition Region Mode Water

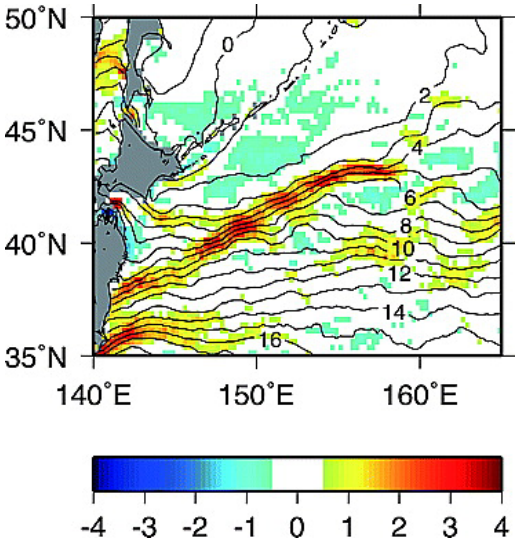

1 of 4

Climate

Three centuries of Myanmar monsoon climate variability inferred from teak tree rings

Rosanne D'Arrigo, Jonathan Palmer, Caroline C. Ummenhofer, Nyi Nyi Kyaw, Paul Krusic

First Published: 24 December 2011 Vol: 38, L24705 | DOI: 10.1029/2011GL049927

KEY POINTS

- Tree-ring chronology for Myanmar
- Identifies unusual nature of recent El Nino
- Identifies large-scale

1 of 3

Hydrology and Land Surface Studies

The rate of fluvial gravel dispersion

Judith K. Haschenburger

First Published: 22 December 2011 Vol: 38, L24403 | DOI: 10.1029/2011GL049928

KEY POINTS

- Gravel dispersion rates decrease over time until limiting values are reached
- Streamwise dispersion rates exceed vertical dispersion rates
- Size-selective grain dispersion persists only in the streamwise component

1 of 3

Oceans

Hypoxia in future climates: A model ensemble study for the Baltic Sea

H. E. M. Meier, H. C. Andersson, K. Eilola, B. G. Gustafsson, I. Kuznetsov, B. Müller-Karulis, T. Neumann, O. P. Savchuk

First Published: 29 December 2011 Vol: 38, L24608 | DOI: 10.1029/2011GL049929

KEY POINTS

- Changing climate will affect the marine environment of the Baltic Sea
- Future hypoxic area will very likely increase or at best slightly decrease
- Response time scales to changing climate and nutrient loads are similar

Open Access

1 of 4

The Cryosphere

Topographic control of asynchronous glacial advances: A case study from Annapurna, Nepal

Beth Pratt-Sitaula, Douglas W. Burbank, Arjun M. Heimsath, Neil F. Humphrey, Michael Oskin, Jaakko Putkonen

First Published: 30 December 2011 Vol: 38, L24502 | DOI: 10.1029/2011GL049940

KEY POINTS

- Glaciers with higher max source areas advance in wider range of climate regimes
- Common practice of assuming synchroneity for similar ELA depressions is flawed
- Largest glacial chronology available for central or western Nepalese Himalaya

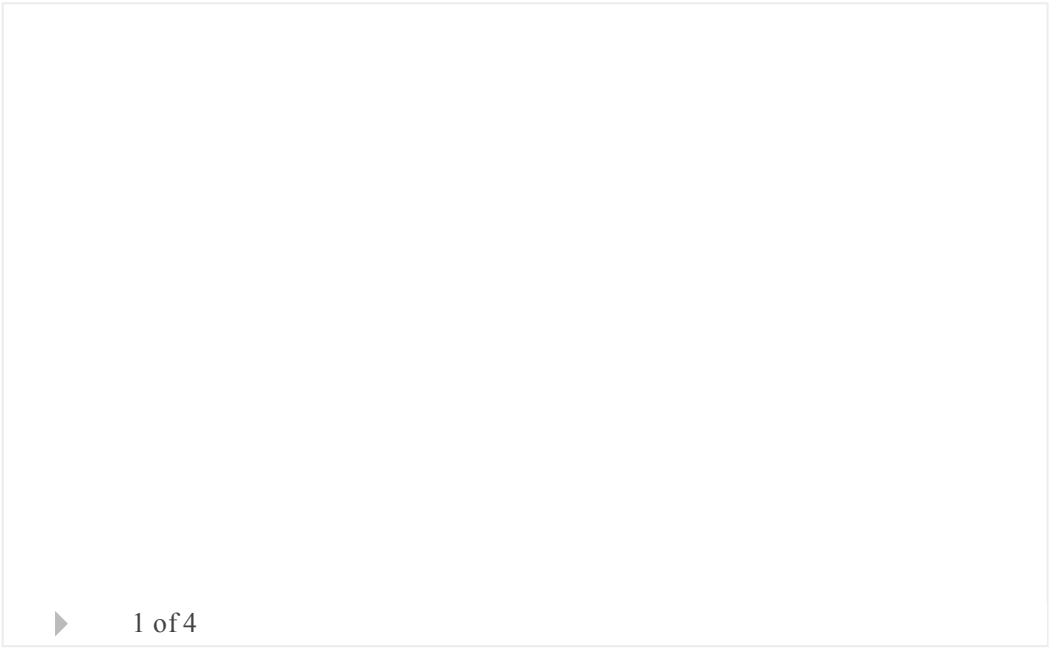

Atmospheric Science

Observations of the initial, upward-propagating, positive leader steps in a rocket-and-wire triggered lightning discharge

Christopher J. Biagi, M. A. Uman, J. D. Hill, D. M. Jordan

First Published: 31 December 2011 Vol: 38, L24809 | DOI: 10.1029/2011GL049944

KEY POINTS

- The upward positive leader is stepped
- The upward positive leader initially is like sparks
- Positive leader step charge and current is measured

1 of 3

Land surface impacts on subseasonal and seasonal predictability

Zhichang Guo, Paul A. Dirmeyer, Tim DelSole

First Published: 29 December 2011 Vol: 38, L24812 | DOI: 10.1029/2011GL049945

KEY POINTS

- Realistically initialized land surface states enhance atmospheric predictability
- The impact of the land surface on atmospheric predictability varies with season
- New mechanisms to explain the temporal evolution of land impacts

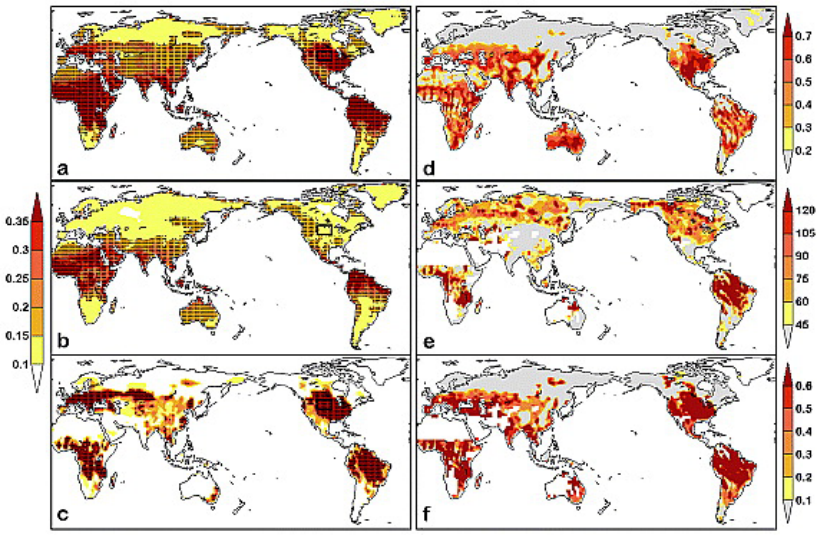

1 of 2

Correction to "Comparisons of satellites liquid water estimates to ECMWF and GMAO analyses, 20th century IPCC AR4 climate simulations, and GCM simulations"

Jui-Lin F. Li, D. E. Waliser, J. H. Jiang

First Published: 23 December 2011 Vol: 38, L24807 | DOI: 10.1029/2011GL049956

Free

1 of 2

The Cryosphere

Traveling supraglacial lakes on George VI Ice Shelf, Antarctica

C. H. LaBarbera, D. R. MacAyeal

First Published: 28 December 2011 Vol: 38, L24501 | DOI: 10.1029/2011GL049970

KEY POINTS

- We discover a type of supraglacial lake that propagates as a wave
- These waves result from large-scale stress regime
- Thus, large-scale stress regime may determine how lakes mediate shelf stability

Highlight

1 of 3

Climate

Correction to "Late 20th century warming and freshening in the central tropical Pacific"

Intan S. Nurhati, Kim M. Cobb, Christopher D. Charles, Robert B. Dunbar

First Published: 29 December 2011 Vol: 38, L24707 | DOI: 10.1029/2011GL049972

Free

Solid Earth

Contribution of satellite gravimetry to understanding seismic source processes of the 2011 Tohoku-Oki earthquake

Shin-Chan Han, Jeanne Sauber, Riccardo Riva

First Published: 29 December 2011 Vol: 38, L24312 | DOI: 10.1029/2011GL049975

KEY POINTS

- The earthquake centroid solution at the lower crust is found
- Fault modeling through gravitational normal modes
- Inversion of new class of earthquake observation for the seismic sources

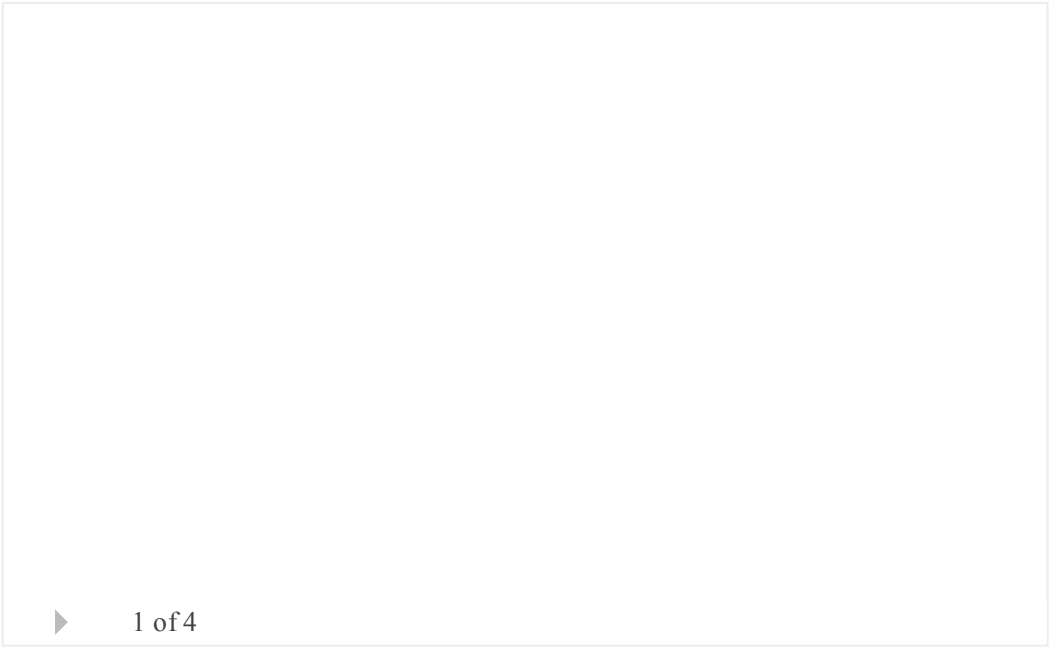

1 of 4

Sound velocities of ferromagnesian carbonates and the seismic detection of carbonates in eclogites and the mantle

Carmen Sanchez-Valle, Sujoy Ghosh, Angelika D. Rosa

First Published: 31 December 2011 Vol: 38, L24315 | DOI: 10.1029/2011GL049981

KEY POINTS

- Elasticity-composition systematics in Mg-Fe carbonates
- Seismic velocities and density of carbonated eclogite and peridotite lithologies
- Implications for the detection of carbonated regions at depth

1 of 3

Climate

Extended warming of the northern high latitudes due to an overshoot of the Atlantic meridional overturning circulation

Peili Wu, Laura Jackson, Anne Pardaens, Nathalie Schaller

First Published: 20 December 2011 Vol: 38, L24704 | DOI: 10.1029/2011GL049998

KEY POINTS

- The AMOC overshoots in response to a CO2 rampdown
- This is due to a build-up of N-S salinity gradient during global warming
- The AMOC overshoot drives an extended warming of the northern high latitudes

1 of 4

Hydrology and Land Surface Studies

Rubber plantations act as water pumps in tropical China

Zheng-Hong Tan, Yi-Ping Zhang, Qing-Hai Song, Wen-Jie Liu, Xiao-Bao Deng, Jian-Wei Tang, Yun Deng, Wen-Jun Zhou, Lian-Yan Yang, Gui-Rui Yu, et al

First Published: 31 December 2011 Vol: 38, L24406 | DOI: 10.1029/2011GL050006

KEY POINTS

- Two independent methods give the same results

- More water was evapotranspirated by rubber plantation than rain forest
- Rubber plantation do act as water pumps

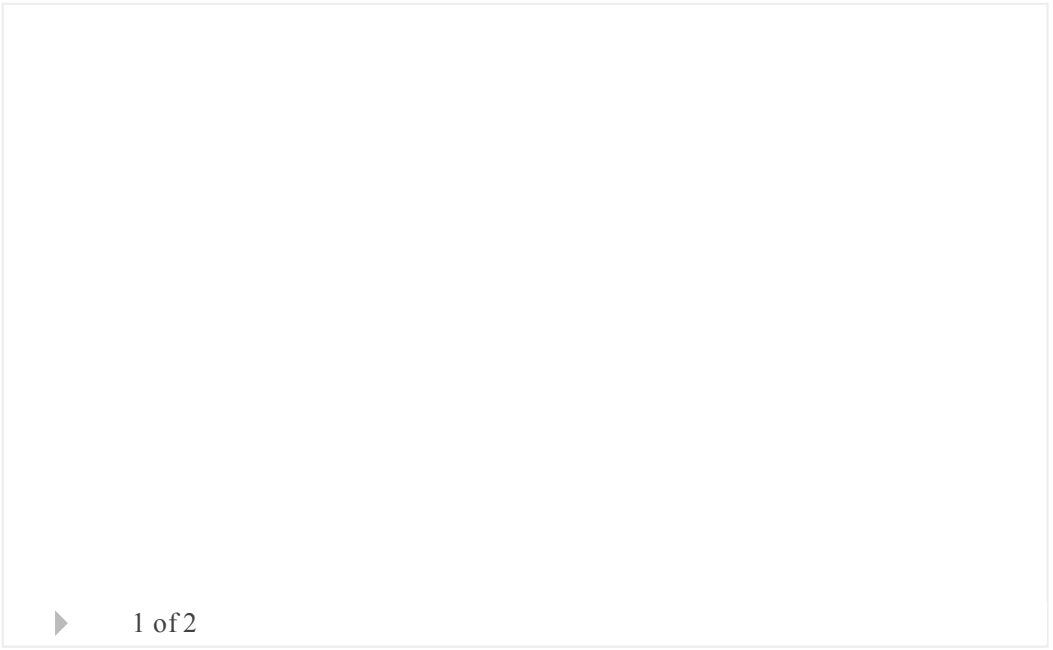

1 of 2

Oceans

Easterly denitrification signal and nitrogen fixation feedback documented in the western Pacific sediments

Guodong Jia, Zhiyang Li

First Published: 24 December 2011 Vol: 38, L24605 | DOI: 10.1029/2011GL050021

KEY POINTS

- Denitrification record in the western equatorial Pacific
- Denitrification signal is not local but advected from eastern tropical Pacific
- Local N2 fixation masks denitrification signals at many western Pacific sites

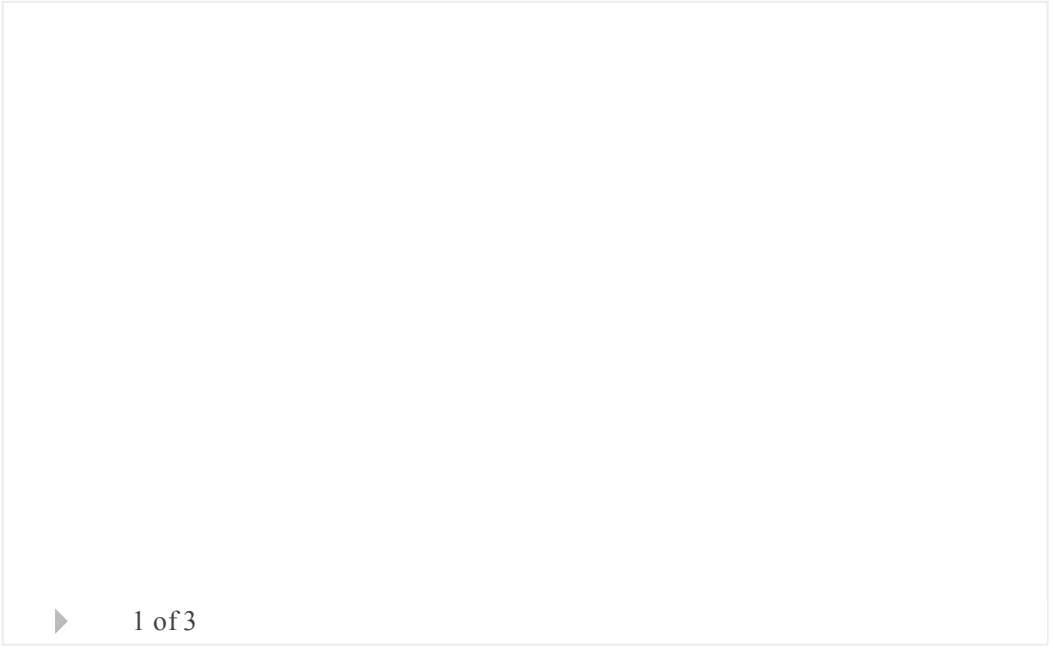

1 of 3

Climate

Tidal mixing around Indonesia and the Maritime continent: Implications for paleoclimate simulations

C. M. Brierley, A. V. Fedorov

First Published: 20 December 2011 Vol: 38, L24703 | DOI: 10.1029/2011GL050027

KEY POINTS

- Tidal mixing within the Maritime continent helps determine climate properties
- Changes in tidal mixing may have changed climate on geological timescales
- Changes in tidal mixing could be the most important aspect of bathymetry changes

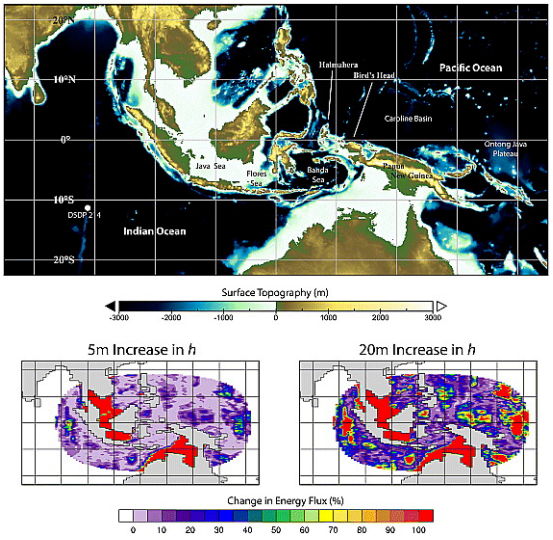

1 of 4

Solid Earth

How pore fluid pressurization influences crack tip processes during dynamic rupture

Nicolas Brantut, James R. Rice

First Published: 30 December 2011 Vol: 38, L24314 | DOI: 10.1029/2011GL050044

KEY POINTS

- The role of flash heating vs thermal pressurization during rupture is studied
- A simplified slip rate profile along a dynamically propagating crack is derived
- For low fracture energy, therm. press. is negligible in the crack cohesive zone

1 of 5

Atmospheric Science

First measurements of thermal tides in the summer mesopause region at Antarctic latitudes

F.-J. Lübken, J. Höffner, T. P. Viehl, B. Kaifler, R. J. Morris

First Published: 28 December 2011 Vol: 38, L24806 | DOI: 10.1029/2011GL050045

KEY POINTS

- First measurements of thermal tides in Antarctica in summer middle atmosphere
- Tidal temperature modulation by up to +/- 6 Kelvin. Up to 40% in Fe density
- Observed tides are much larger compared to models

1 of 4

Solid Earth

Trench-normal variation in observed seafloor displacements associated with the 2011 Tohoku-Oki earthquake

M. Kido, Y. Osada, H. Fujimoto, R. Hino, Y. Ito

First Published: 17 December 2011 Vol: 38, L24303 | DOI: 10.1029/2011GL050057

KEY POINTS

- We observed the largest displacement at closest site to the trench ever reported
- We found strong trench-normal variation in the displacement toward the trench
- We provide definite evidence that the slip extended to the trench

1 of 3

Atmospheric Science

Cloud features detected by MODIS but not by CloudSat and CALIOP

Mark Aaron Chan, Josefino C. Comiso

First Published: 30 December 2011 Vol: 38, L24813 | DOI: 10.1029/2011GL050063

KEY POINTS

- Some clouds observed by MODIS are not detected by CloudSat and CALIOP
- Clouds not detected are primarily low level clouds that are geometrically thin
- Undetected clouds have optical thickness less than 14 and heights below 2.5 km

Open Access

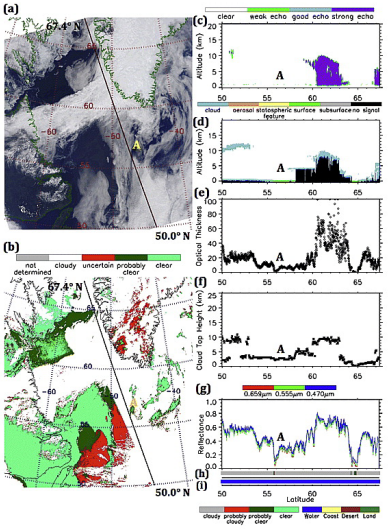

1 of 4

Space Sciences

Constraints on dust production in the Edgeworth-Kuiper Belt from Pioneer 10 and New Horizons measurements

Dong Han, Andrew R. Poppe, Marcus Piquette, Eberhard Grün, Mihály Horányi

First Published: 28 December 2011 Vol: 38, L24102 | DOI: 10.1029/2011GL050136

KEY POINTS

- Dust grains produced in the Kuiper Belt migrate inward
- Dynamical dust grain tracing code is used to establish relative dust densities
- Measurements by Pioneer 10 and New Horizons constrain dust production rates

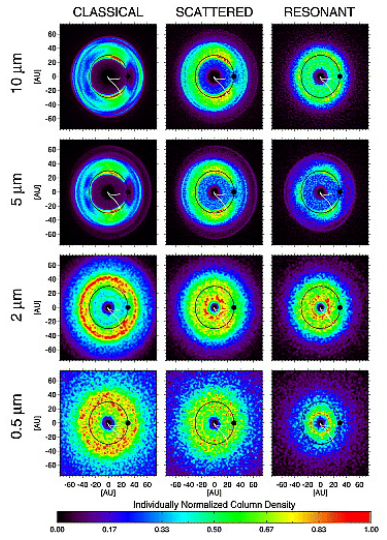

1 of 3

Hydrology and Land Surface Studies

Mobility control through spontaneous formation of nanoparticle stabilized emulsions

D. A. DiCarlo, B. Aminzadeh, M. Roberts, D. H. Chung, S. L. Bryant, C. Huh

First Published: 30 December 2011 Vol: 38, L24404 | DOI: 10.1029/2011GL050147

KEY POINTS

- Emplaced nanoparticles change the pattern of injected nonaqueous phase
- Patterns change as emulsion is created in-situ even at low flow rates
- Nanoparticles effectively slow down propagation of nonaqueous phase

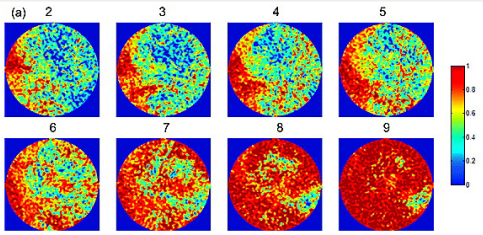

1 of 3

The role of eddies inside pores in the transition from Darcy to Forchheimer flows

Kuldeep Chaudhary, M. Bayani Cardenas, Wen Deng, Philip C. Bennett

First Published: 30 December 2011 Vol: 38, L24405 | DOI: 10.1029/2011GL050214

KEY POINTS

- The Darcy law fails due to growth of pre-existing eddies inside pores
- Decrease in apparent hydraulic conductivity is due to narrowing of flow channel
- Forchheimer flow characteristics are due to growth behavior of eddies in pores

1 of 4

Space Sciences

Post-equinox periodicities in Saturn's energetic electrons

J. F. Carbary, D. G. Mitchell, S. M. Krimigis, N. Krupp

First Published: 24 December 2011 Vol: 38, L24104 | DOI: 10.1029/2011GL050259

KEY POINTS

- Saturn magnetospheric period evolves from single to multiple to none
- Changes in period may be related to change in orbit from dusk to dayside
- Magnetospheric periodicity at Saturn may depend on local time

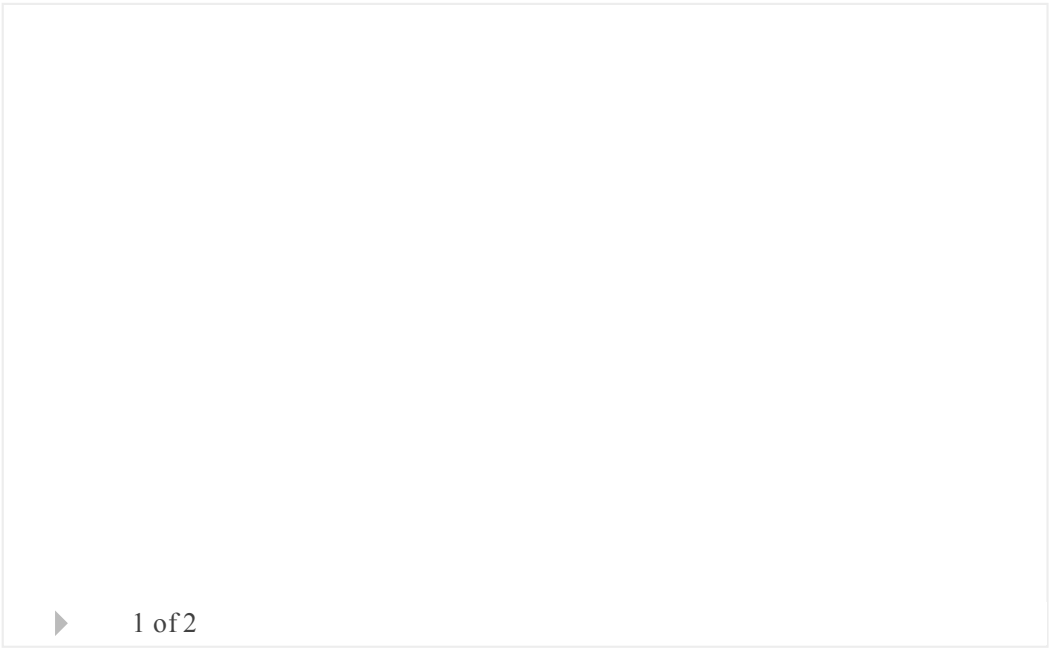

1 of 2

Planets

Tidal variations in the Martian lower atmosphere inferred from Mars Express Planetary Fourier Spectrometer temperature data

T. M. Sato, H. Fujiwara, Y. O. Takahashi, Y. Kasaba, V. Formisano, M. Giuranna, D. Grassi

First Published: 29 December 2011 Vol: 38, L24205 | DOI: 10.1029/2011GL050348

KEY POINTS

- Latitudinal and diurnal temperature variations are consistent with GCM results
- Diurnal variations in the tropics are explained by the migrating diurnal tide
- The wave-3 structure caused by DK2 is dominated at altitude of ~40 km

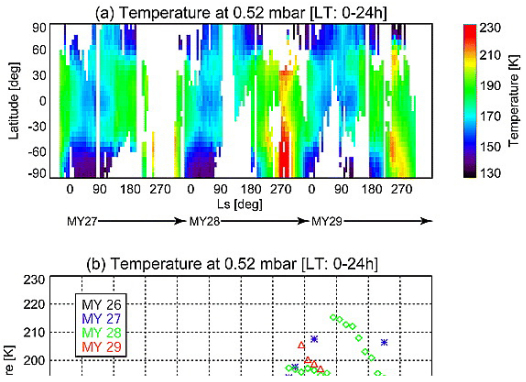

1 of 3

Current Issue

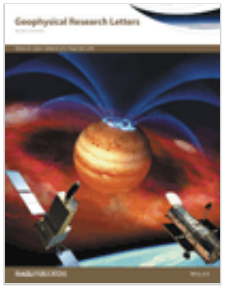

Volume 42
Issue 6
28 March 2015

All Issues
Browse a free sample issue

Find an article

and

or

Stay Connected to Eos

Journal Resources

Call for Papers

Special Section Proposal Form

Personal Choice

Terms of Use

Cover Gallery

Institutional Subscription Rates

Get RSS Feed

Featured Special Collection

The Early Results from the Van Allen Probes

NASA's Van Allen Probes mission is designed to acquire data to solve key questions

about the energetics and dynamics of the Earth's Van Allen Radiation belts that have arisen from active research in the domain in the past decades.

Editors' Highlights

- **What Causes Sunspot Pairs?**
- **Water Beneath the Surface of Mars, Bound up in Sulfates**
- **When Predicting Drought Risk, Do Not Overlook Temperature**
- **Changing Patterns in U.S. Air Quality**

See all »

Download the app

Download the Geophysical Research Letters app on your iPad

Upcoming AGU Meetings

Triennial Earth-Sun Summit

26 Apr - 1 May 2015
Indianapolis, Indiana, USA

2015 Joint Assembly

3-7 May 2015
Montreal, Canada

Chapman Conference on Evolution of the Asian Monsoon and its Impact on Landscape, Environment and Society: Using the Past as the Key to the Future

14-19 June 2015
Hong Kong SAR, China

See all »